Author(s): Mears, Kristian L.; Nguyen, Gia-Ann; Ruiz, Bronson; Lehmann, Annika; Nelson, Jonah; Fettinger, James C.; Tuononen, Heikki M.; Power, Philip P.

Title: Hydrobismuthation : Insertion of Unsaturated Hydrocarbons into the Heaviest Main Group Element Bond to Hydrogen

Year: 2024

Version: Published version

Please cite the original version:

Mears, K. L., Nguyen, G.-A., Ruiz, B., Lehmann, A., Nelson, J., Fettinger, J. C., Tuononen, H. M., & Power, P. P. (2024). Hydrobismuthation : Insertion of Unsaturated Hydrocarbons into the Heaviest Main Group Element Bond to Hydrogen. Journal of the American Chemical Society, 146(1), 19-23. https://doi.org/10.1021/jacs.3c06535

JACS
JOURNAL OF THE AMERICAN CHEMICAL SOCIETY

pubs.acs.org/JACS
Communication

Hydrobismuthation: Insertion of Unsaturated Hydrocarbons into the Heaviest Main Group Element Bond to Hydrogen

Kristian L. Mears, Gia-Ann Nguyen,‖ Bronson Ruiz,‖ Annika Lehmann,‖ Jonah Nelson,‖ James C. Fettinger, Heikki M. Tuononen,* and Philip P. Power*

Cite This: https://doi.org/10.1021/jacs.3c06535

ABSTRACT: The bismuth hydride $(2,6\text{-}Mes_2H_3C_6)_2BiH$ (**1**, Mes = 2,4,6-trimethylphenyl), which has a Bi−H ^1H NMR spectroscopic signal at δ = 19.64 ppm, was reacted with phenylacetylene at 60 °C in toluene to yield $[(2,6\text{-}Mes_2C_6H_3)_2BiC(Ph)=CH_2]$ (**2**) after 15 min. Compound **2** was characterized by ^1H, ^{13}C NMR, and UV−vis spectroscopy, single crystal X-ray crystallography, and calculations employing density functional theory. Compound **2** is the first example of a hydrobismuthation addition product and displays Markovnikov regioselectivity. Computational methods indicated that it forms via a radical mechanism with an associated Gibbs energy of activation of 91 kJ mol^{-1} and a reaction energy of −90 kJ mol^{-1}.

The reactivity and use of bismuth and its derivatives in synthesis and catalysis have undergone a renaissance that owes much to the work of Cornella and co-workers.[1] The redox active nature of this heavy main group element has recently been exploited in various chemical transformations, including radical activation and coupling of redox-active electrophiles,[2,3] aryl−F bond formation,[4,5] and transfer hydrogenation catalysis.[6,7] The last example is of particular interest to us since preliminary mechanistic investigations implicated the involvement of an elusive bismuth hydride, namely, **I** (Figure 1). More detailed studies provided a comprehensive mechanistic picture that explained the ability of bismuth to perform transformations typical for transition metals and allowed the realization of better, second-generation, catalysts with improved properties.

Currently, the reactivity of bismuth hydrides is virtually undeveloped due to the perceived instability of the [Bi−H] unit. The parent bismuthine, **II** (Figure 1, IUPAC name, bismuthane), was first synthesized by Amberger[8] in 1961 and characterized by Bürger in 2002.[9] It decomposes to metallic bismuth and gaseous dihydrogen at temperatures well below 0 °C. In 2002, Breunig and co-workers reported a dialkyl bismuth hydride of the formula $[Bi(H)(CH\{SiMe_3\}_2)_2]$, **III** (Figure 1).[10] It was found to be thermally sensitive and readily converted to the corresponding alkyl dibismuthane $[Bi(CH\{SiMe_3\}_2)_2]_2$ at room temperature via the release of dihydrogen gas. To date, the only thermally stable complex containing a Bi−H bond is $[Bi(H)(2,6\text{-}Mes_2C_6H_3)_2]$, **1** (Mes = 2,4,6-trimethylphenyl, Figure 1), synthesized by us in 2000.[11] In this species, the [Bi−H] unit is protected by two kinetically stabilizing terphenyl ligands, although the bulky mesityl groups do not completely block reactivity and samples of solid **1** convert to purple dibismuthene $[Bi(2,6\text{-}Mes_2C_6H_3)]_2$ at temperatures >130 °C via loss of terphenyl arene $2,6\text{-}Mes_2C_6H_4$ and subsequent dimerization of $[Bi(2,6\text{-}Mes_2C_6H_3)]$.[12,13]

Because **1** is the only compound with a [Bi−H] unit that is kinetically stable at room temperature, we hypothesized that it could perform hydrometalation of unsaturated organic substrates such as acetylenes and olefins. Similar hydroaddition reactions are known for other heavier pnictogens (Figure 1, bottom). For example, hydrophosphinations employing both catalyst[14,17] and catalyst-free[18] strategies have been reported, with more recent advances focused on the use of the parent phosphine in synthesis.[19] Hydroarsinations are known to take place in the presence of Zr-cocatalysts,[15] while the first example of an antimony hydride capable of a hydrostibination of alkynes, alkenes, and other substrates was reported by Chitnis and co-workers in 2019.[16] Herein, we report the first instance of a hydrobismuthation; this involves the reaction of **1** and phenylacetylene, which results in the Markovnikov addition product **2** $[(2,6\text{-}Mes_2C_6H_3)_2BiC(Ph)=CH_2]$ (Figure 1, bottom).

Compound **2** was isolated in high yield (83%) as an orange powder after the removal of all volatile components. Orange-yellow block-like crystals suitable for analysis by single crystal X-ray diffraction could be grown from a concentrated hexane solution of the powder at room temperature. The crystal structure of **2** (Figure 2) was found to possess approximately 8% disorder as refined for the bismuth atom, which presumably involving the two different orientations possible for the $PhC=CH_2$ fragment. However, the minor component of the structure could not be located for the lighter carbon atoms, for which they were refined with site occupancy factors equal to unity.

Received: June 20, 2023
Revised: December 15, 2023
Accepted: December 18, 2023

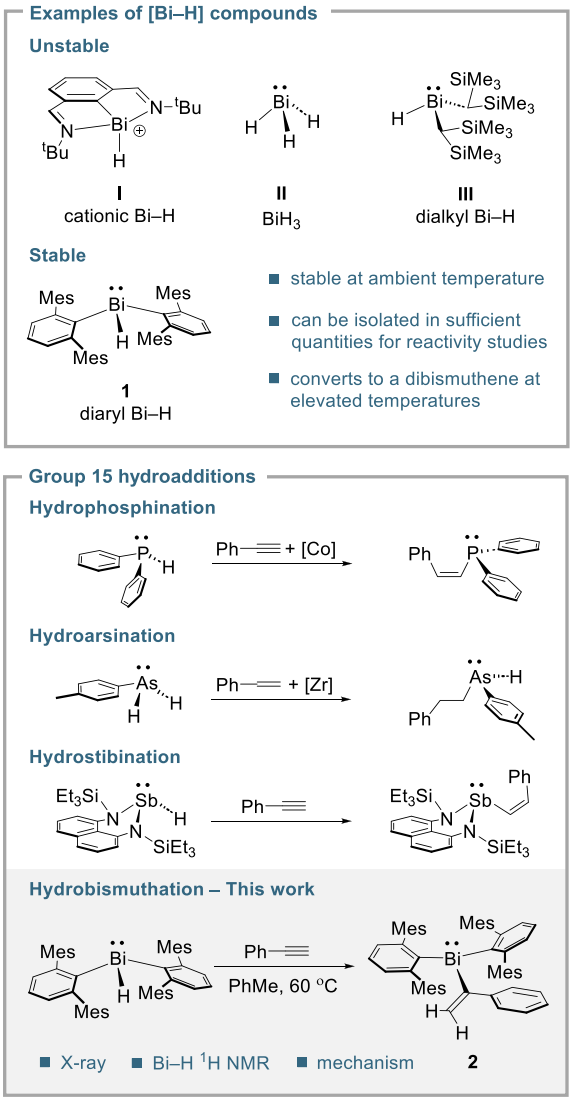

Figure 1. Examples of [Bi–H] compounds (top)[6,8,10,11] and group 15 hydroadditions (bottom),[14−16] including the hydrobismuthation reaction reported herein.

The structure of **2** displays a C(1)−C(2) bond length of 1.321(9) Å, in good agreement with a reference C=C bond length of 1.34 Å from Pyykkö covalent radii.[20] At 2.286(6) Å, the Bi(1)−C(2) bond length matches the sum of single bond covalent radii for carbon and bismuth, 2.26 Å,[20] and is statistically identical to a Bi−C bond in **IV**, 2.289(4) Å (Figure 3); the Bi−C bond in **2** is also comparable to related single bonds in compounds where bismuth is three-coordinate and the carbon atom belongs to a conjugated system, such as **V** and **VI** at 2.260(4) and 2.293(3) Å, respectively.[21−23] The three C−Bi−C bond angles in **2** are dissimilar; with values of 89.2(2)°, 101.2(2)°, and 128.1(2)°, for a sum of 318.5(2)°, consistent with trigonal pyramidal geometry at bismuth. The two Bi···π arene centroid distances are 3.498 and 3.910 Å, of which the former suggests the presence of a significant intramolecular dispersion component. Interestingly, the structure of **2** shows that the reaction has taken place with Markovnikov regioselectivity, while the recent example of a catalyst-free hydrostibination occurred with anti-Markovnikov selectivity.[16]

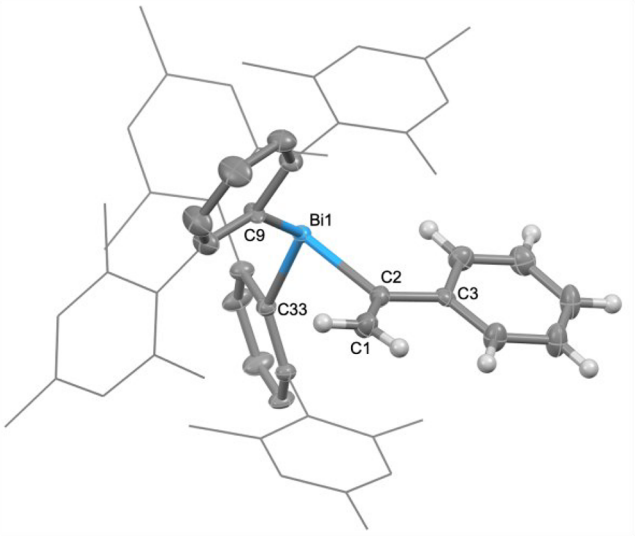

Figure 2. Single crystal X-ray structure of complex **2** with carbon atoms of the mesityl groups shown in wireframe format and hydrogen atoms not shown.Thermal ellipsoids are drawn at 50% probability level. Selected bond lengths (Å) and angles (deg): C(1)−C(2) = 1.321(9), Bi(1)−C(2) = 2.286(8), C(9)−Bi(1)−C(2) = 89.2(2), C(2)−Bi(1)−C(33) = 101.2(2), and C(2)−Bi(1)−C(9) = 128.1(2).

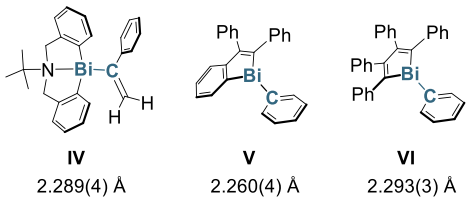

Figure 3. Examples of Bi−C bond lengths in compounds **IV**−**VI** for comparison with the Bi(1)−C(2) bond length. of 2.286(6) Å in **2**.[21−23]

The ^{1}H NMR spectrum of **2** in C_6D_6 shows the expected signals, including two broad singlets at $\delta(^1H)$ = 8.49 and 6.20 ppm that were assigned to the vinylic protons of the PhC=CH_2 fragment. Such a large difference between the two chemical shifts can be explained by the distance of these nuclei from the heavy bismuth atom, the proton closer being more shielded and therefore shifted more upfield. While ^{1}H DOSY confirmed that the two singlets originate from the same species, neither ^{1}H−^{1}H COSY nor ^{1}H−^{13}C HSQC provided any additional information. The UV−vis spectrum of **2** in hexanes showed a broad singlet in the UV-A area (λ_{max} = 321 nm), which is consistent with the spectral characteristics of *m*-terphenyl ligands.

Even though the single-crystal X-ray data originally reported for **1** showed signals consistent with a disordered hydrogen atom at 1.94(2) Å bonded to bismuth, the reliability of the assignment is limited. Furthermore, no ^{1}H NMR signal could be detected for the hydridic proton at the time, and the presence of a [Bi−H] unit was inferred from a strong IR absorption band at 1759 cm^{-1} along with its isotopic shift upon deuterium exchange. A computational (PBE1PBE-D3BJ/def2-TZVP) optimization of the structure of **1** using density functional theory (DFT) gave a Bi−H bond length of 1.778 Å and a scaled Bi−H stretch at 1807 cm^{-1}, while an NMR signal corresponding to the hydridic proton was located at $\delta(^1H)$ = 19.64 ppm by employing a wider scanning window. Despite

https://doi.org/10.1021/jacs.3c06535
J. Am. Chem. Soc. XXXX, XXX, XXX−XXX

the large quadrupole moment of the ^{209}Bi nucleus (100%, I = $^{9}/_{2}$, Q = −420(17) mb),[24] the NMR signal is well resolved. The observed chemical shift is in excellent agreement with high-level theoretical predictions by Straka, Kaupp, and Marek,[25] who calculated $\delta(^1H)$ = 19.4 ppm for **1** using a four-component Dirac−Kohn−Sham approach that includes important spin−orbit effects largely responsible for the observed chemical shift ($\delta^{SO}(^1H)$ = 14.4 ppm). For comparison, complex **III** (the only other bismuth hydride for which NMR data are available) shows a broad ^{1}H signal with $\delta(^1H)$ = 3.24 ppm, which compares well with the theoretical chemical shift $\delta(^1H)$ = 2.1 ppm ($\delta^{SO}(^1H)$ = 0.7 ppm) reported for the simple alkyl bismuth hydride Bi(H)$(CH_3)_2$.[25]

The mechanism for hydrobismuthation was examined with DFT. Similarly to the results of Chitnis and co-workers for hydrostibination,[26] all closed-shell pathways leading to **2** were found to have significant energy barriers and are, therefore, unfeasible under the experimental conditions. Consequently, a radical mechanism was sought, which led to the characterization of transition states **TS-1** for hydrogen transfer from **1** to phenylacetylene (Figure 4). The Gibbs energy of activation for

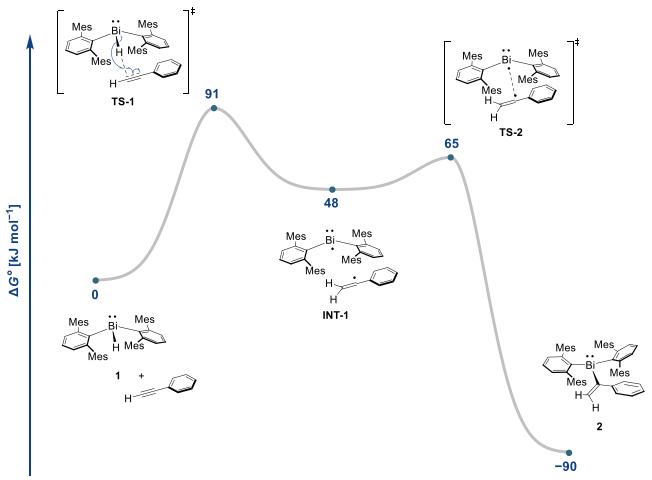

Figure 4. Calculated mechanism for the formation of **2**. Relative Gibbs energies refer to gas phase calculations at room temperature.

this process was found to be 91 kJ mol^{-1} at room temperature. The bismuthinyl and 1-phenylvinyl radicals thus formed were found to associate to a weakly bound intermediate **INT-1** that resides 48 kJ mol^{-1} higher in energy than the starting species. The Gibbs energy of activation for radical recombination through **TS-2** was found to be 17 kJ mol^{-1}, giving **2** with a relative Gibbs energy of −90 kJ mol^{-1}.

In contrast the mechanism for hydrostibination follows a pathway in which the stibinyl and 1-phenylvinyl radicals separate, allowing the former to add to an equivalent of phenylacetylene and undergo a second hydrogen transfer to give the anti-Markovnikov product.[26] In this context, the dissociation of **INT-1** to bismuthinyl and 1-phenylvinyl radicals was calculated to be an entropy-driven process, while the transition state associated with the addition of the bismuthinyl radical to phenylacetylene was found to be energetically on par with **TS-1**. Thus, the recombination of bismuthinyl and 1-phenylvinyl radicals, as shown in Figure 4, represents the minimum energy pathway and agrees with the observed Markovnikov regioselectivity. We hypothesize that the difference in regioselectivity between antimony and bismuth originates from the different steric protection around the group 15 element, which, in the case of **1** contributes to the stability of **INT-1** and allows facile formation of **2** rather than separation of the radicals by an intervening molecule of phenylacetylene.

Encouraged by the favorable reactivity of **1** with phenylacetylene, we attempted the activation of other important substrates, such as olefins. Recently, Cornella and co-workers reported the only known activation of ethylene with a heavy pnictogen species by coordinating it to a distibene which formed a stibacyclopropane upon dissociation.[27] In our case, an ampule containing **1** dissolved in toluene was saturated with ethylene gas using the standard freeze−pump−thaw method. The mixture was heated to 60 °C, which resulted in the initially colorless solution turning slightly yellow. A pale-yellow powder was obtained upon removal of all volatiles, which was dissolved in hexane and filtered. Over 12 h, the solution became an intense dark purple color, indicating the formation of dibismuthene [Bi(2,6-$Mes_2C_6H_3$)]$_2$.

Repeating the reaction of **1** with ethylene in a J. Young tube allowed its *in situ* monitoring with ^{1}H NMR spectroscopy (Figure 5). This revealed that **1** does not add to ethylene at

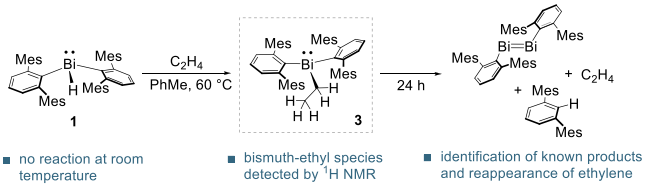

Figure 5. Synthetic route to bismuth-ethyl species **3** and the identified side-products.

room temperature, but the [Bi−H] signal disappears within 15 min at 60 °C. A ^{1}H NMR spectrum of the reaction mixture showed quartet and triplet signals at δ = 3.27 ppm ($^3J_{HH}$ = 7.0 Hz) and 1.12 ppm ($^3J_{HH}$ = 7.0 Hz), respectively, corresponding to the CH_2 and CH_3 moieties of a putatively assigned ethyl group, suggesting the formation of **3** [(2,6-$Mes_2C_6H_3$)$_2$BiC(H)$_2$$CH_3$], albeit in low yield. Removal of unreacted ethylene under reduced pressure and allowing the sample to remain in C_6D_6 for 24 h permitted the identification of dibismuthene [Bi(2,6-$Mes_2C_6H_3$)]$_2$ and terphenyl arene 2,6-$Mes_2C_6H_4$, by^{1}H NMR spectroscopy. Interestingly, reappearance of ethylene was also observed by ^{1}H NMR spectroscopy, possibly owing to decomposition of **3**, although this is not readily apparent from the spectral data.

The reaction of **1** with ethylene was examined with DFT (Figure 6). The Gibbs energy of activation for hydrogen transfer from **1** to ethylene was found to be 116 kJ mol^{-1} at room temperature, which is in agreement with the stability of **1** under these conditions. Compound **3** was found to be only 36 kJ mol^{-1} more stable than the reactants, and no low-energy pathway could be identified for its decomposition. In contrast, the decomposition of **1** was found to have a Gibbs energy of activation of 113 kJ mol^{-1} and, in the presence of ethylene, was found to give bismacyclopropane [(C_2H_4)Bi(2,6-$Mes_2C_6H_3$)] and terphenyl arene 2,6-$Mes_2C_6H_4$. Subsequent dissociation of bismacyclopropane would not only provide a pathway to dibismuthene [Bi(2,6-$Mes_2C_6H_3$)]$_2$ (dimerization) but would also explain the reappearance of ethylene seen by ^{1}H NMR. At this point, the exact details of the reaction remain unknown, and no experimental evidence for the intermediacy of

https://doi.org/10.1021/jacs.3c06535
J. Am. Chem. Soc. XXXX, XXX, XXX−XXX

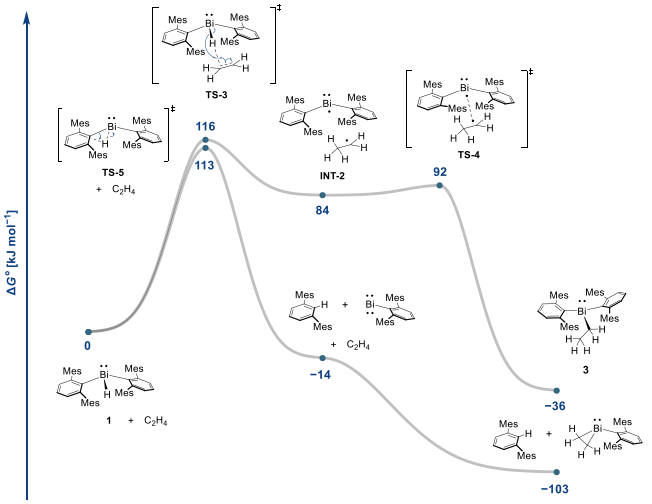

Figure 6. Calculated mechanisms for the formation of **3** and dissociation of **1**. Relative Gibbs energies refer to gas phase calculations at room temperature. The energy of **TS-4** was estimated based on a potential energy surface scan (see Supporting Information for details).

bismacyclopropane exists. However, computational modeling of possible pathways clearly shows that ethylene is a poor substrate for hydrobismuthation because the formation of **3** is equally likely as is the decomposition of **1**, leading to a mixture of products.

In conclusion, we have reported a ^{1}H NMR chemical shift (δ = 19.64 ppm) for the hydrogen of a Bi−H bond in [Bi(H)(2,6-$Mes_2C_6H_3$)$_2$] (**1**), which is in excellent agreement with a previous computational prediction (δ = 19.4 ppm). We have also reported the first example of hydrobismuthation involving the addition of phenylacetylene to **1** at 60 °C in toluene. The reaction occurred with Markovnikov regioselectivity and gave [(2,6-$Mes_2C_6H_3$)$_2$BiC(Ph)=CH_2] (**2**). Density functional theory calculations support a radical mechanism, whereby hydrogen transfer from **1** to phenylacetylene generates bismuthinyl and 1-phenylvinyl radicals that rapidly recombine to form **2**. We further attempted the hydrobismuthation of ethylene with **1**. At elevated temperatures, the reaction mixture potentially generates small amounts of the bismuth-ethyl species [(2,6-$Mes_2C_6H_3$)$_2$BiC(H)$_2$$CH_3$] (**3**), though dibismuthene [Bi(2,6-$Mes_2C_6H_3$)] and terphenyl arene were also identified along with regeneration of ethylene. Computational analysis of possible reaction pathways indicated that ethylene is a poor substrate for hydrobismuthation, as the barrier for its addition to **1** is similar to that associated with the decomposition of **1**. The investigation of hydrobismuthation insertions of other unsaturated organic substrates is continuing. The results add further support to the notion that even the heaviest main group metal hydrides can have a rich chemistry.[28]

■ ASSOCIATED CONTENT

Supporting Information

The Supporting Information is available free of charge at https://pubs.acs.org/doi/10.1021/jacs.3c06535.

Experimental and characterization details for all new compounds, including full spectroscopic and crystallographic data, as well as full computational details and optimized structures (*xyz*-coordinates). (PDF)

Accession Codes

CCDC 2269746 contains the supplementary crystallographic data for this paper. These data can be obtained free of charge via www.ccdc.cam.ac.uk/data_request/cif, or by emailing data_request@ccdc.cam.ac.uk, or by contacting The Cambridge Crystallographic Data Centre, 12 Union Road, Cambridge CB2 1EZ, UK; fax: +44 1223 336033.

■ AUTHOR INFORMATION

Corresponding Authors

Philip P. Power − *Department of Chemistry, University of California, Davis, California 95616, United States;* orcid.org/0000-0002-6262-3209; Email: pppower@ucdavis.edu

Heikki M. Tuononen − *Department of Chemistry, NanoScience Centre, University of Jyväskylä, FI-40140 Jyväskylä, Finland;* orcid.org/0000-0002-4820-979X; Email: heikki.m.tuononen@jyu.fi

Authors

Kristian L. Mears − *Department of Chemistry, University of California, Davis, California 95616, United States;* orcid.org/0000-0002-8515-4177

Gia-Ann Nguyen − *Department of Chemistry, University of California, Davis, California 95616, United States*

Bronson Ruiz − *Department of Chemistry, University of California, Davis, California 95616, United States*

Annika Lehmann − *Department of Chemistry, NanoScience Centre, University of Jyväskylä, FI-40140 Jyväskylä, Finland;* orcid.org/0000-0003-1775-9163

Jonah Nelson − *Department of Chemistry, NanoScience Centre, University of Jyväskylä, FI-40140 Jyväskylä, Finland; Department of Chemistry, University of Calgary, Calgary, Alberta, Canada T2N 1N4*

James C. Fettinger − *Department of Chemistry, University of California, Davis, California 95616, United States;* orcid.org/0000-0002-6428-4909

Complete contact information is available at: https://pubs.acs.org/10.1021/jacs.3c06535

Author Contributions

‖G.-A.N., B.R., A.L., and J.N. contributed equally.

Funding

United States National Science Foundation Grant Nos. CHE-2152760 and CHE-1531193. European Research Council, Horizon 2020 Programme Grant No. 772510.

Notes

The authors declare no competing financial interest.

■ ACKNOWLEDGMENTS

We thank the U.S. National Science Foundation for funding (Grant No. CHE-2152760) and for the purchase of a dual-source X-ray diffractometer (Grant No. CHE-1531193). The project received funding from the European Research Council under the EU's Horizon 2020 Programme (Grant #772510). Computational resources were provided by the Finnish Grid and Cloud Infrastructure (persistent identifier urn:nbn:fi:research-infras-2016072533).

REFERENCES

(1) Moon, H. W.; Cornella, J. Bismuth Redox Catalysis: An Emerging Main-Group Platform for Organic Synthesis. *ACS Catal.* **2022**, *12*, 1382−1393.

(2) Yang, X.; Reijerse, E. J.; Bhattacharyya, K.; Leutzsch, M.; Kochius, M.; Nöthling, N.; Busch, J.; Schnegg, A.; Auer, A. A.; Cornella, J. Radical Activation of N−H and O−H Bonds at Bismuth(II). *J. Am. Chem. Soc.* **2022**, *144*, 16535−16544.

(3) Mato, M.; Spinnato, D.; Leutzsch, M.; Moon, H. W.; Reijerse, E. J.; Cornella, J. Bismuth radical catalysis in the activation and coupling of redox-active electrophiles. *Nat. Chem.* **2023**, *15*, 1138−1145.

(4) Planas, O.; Wang, F.; Leutzsch, M.; Cornella, J. Fluorination of arylboronic esters enabled by bismuth redox catalysis. *Science* **2020**, *367* (6475), 313−317.

(5) Planas, O.; Peciukenas, V.; Leutzsch, M.; Nöthling, N.; Pantazis, D. A.; Cornella, J. Mechanism of the Aryl−F Bond-Forming Step from Bi(V) Fluorides. *J. Am. Chem. Soc.* **2022**, *144*, 14489−14504.

(6) Wang, F.; Planas, O.; Cornella, J. Bi(I)-Catalyzed Transfer-Hydrogenation with Ammonia-Borane. *J. Am. Chem. Soc.* **2019**, *141*, 4235−4240.

(7) Moon, H. W.; Wang, F.; Bhattacharyya, K.; Planas, O.; Leutzsch, M.; Nöthling, N.; Auer, A. A.; Cornella, J. Mechanistic Studies on the Bismuth-Catalyzed Transfer Hydrogenation of Azoarenes. *Angew. Chem., Int. Ed.* **2023**, *62*, e202313578.

(8) Amberger, E. Hydride Des Wismuts. *Chem. Ber.* **1961**, *94* (6), 1447−1452.

(9) Jerzembeck, W.; Burger, H.; Constantin, L.; Margules, L.; Demaison, J.; Breidung, J.; Thiel, W. Bismuthine BiH_3: Fact or Fiction? High-Resolution Infrared, Millimeter-Wave, and Ab Initio Studies. *Angew. Chem., Int. Ed.* **2002**, *41*, 2550−2552.

(10) Balázs, G.; Breunig, H. J.; Lork, E. Synthesis and Characterization of R_2SbH, R_2BiH, and $R_2Bi{-}BiR_2$ [R = $(Me_3Si)_2CH$]. *Organometallics* **2002**, *21*, 2584−2586.

(11) Hardman, N. J.; Twamley, B.; Power, P. P. $(2,6\text{-}Mes_2H_3C_6)_2BiH$, a Stable, Molecular Hydride of a Main Group Element of the Sixth Period, and Its Conversion to the Dibismuthene $(2,6\text{-}Me_{s2}H_3C_6)BiBi(2,6\text{-}Mes_2C_6H_3)$. *Angew. Chem., Int. Ed.* **2000**, *39*, 2771−2773.

(12) Ellis, B. D.; Macdonald, C. L. B. Stable compounds containing heavier group 15 elements in the + 1 oxidation State. *Coord. Chem. Rev.* **2007**, *251*, 936−973.

(13) Twamley, B.; Sofield, C. D.; Olmstead, M. M.; Power, P. P. Homologous Series of Heavier Element Dipnictenes $2,6\text{-}Ar_2H_3C_6E$ = $EC_6H_3\text{-}2,6\text{-}Ar_2$ (E = P, As, Sb, Bi; Ar = Mes = $C_6H_2\text{-}2,4,6\text{-}Me_3$; or Trip = $C_6H_2\text{-}2,4,6\text{-}{}^{i}Pr_3$) Stabilized by *m*-Terphenyl Ligands. *J. Am. Chem. Soc.* **1999**, *121*, 3357−3367.

(14) Kumar, P.; Sen, A.; Rajaraman, G.; Shanmugam, M. An unusual mixed-valence cobalt dimer as a catalyst for the anti-markovnikov hydrophosphination of alkynes. *Inorg. Chem. Front.* **2022**, *9* (10), 2161−2172.

(15) Bange, C. A.; Waterman, R. Zirconium-catalyzed hydroarsination with primary arsines. *Polyhedron* **2018**, *156*, 31−34.

(16) Marczenko, K. M.; Zurakowski, J. A.; Bamford, K. L.; MacMillan, J. W. M.; Chitnis, S. S. Hydrostibination. *Angew. Chem., Int. Ed.* **2019**, *58*, 18096−18101.

(17) Espinal-Viguri, M.; King, A. K.; Lowe, J. P.; Mahon, M. F.; Webster, R. L. Hydrophosphination of Unactivated Alkenes and Alkynes Using Iron(II): Catalysis and Mechanistic Insight. *ACS Catal.* **2016**, *6*, 7892−7897.

(18) Bissessar, D.; Egly, J.; Achard, T.; Steffanut, P.; Bellemin-Laponnaz, S. Catalyst-free hydrophosphination of alkenes in presence of 2-methyltetrahydrofuran: a green and easy access to a wide range of tertiary phosphines. *RSC Adv.* **2019**, *9*, 27250−27256.

(19) Hood, T. M.; Lau, S.; Webster, R. L. Taming PH_3: State of the Art and Future Directions in Synthesis. *J. Am. Chem. Soc.* **2022**, *144*, 16684−16697.

(20) Pyykkö, P.; Atsumi, M. Molecular Double-Bond Covalent Radii for Elements Li−E112. *Chem.—Eur. J.* **2009**, *15*, 12770−12779.

(21) Parke, S. M.; Hupf, E.; Matharu, G. K.; de Aguiar, I.; Xu, L.; Yu, H.; Boone, M. P.; de Souza, G. L. C.; McDonald, R.; Ferguson, M. J.; He, G.; Brown, A.; Rivard, E. Aerobic Solid State Red Phosphorescence from Benzobismole Monomers and Patternable Self-Assembled Block Copolymers. *Angew. Chem., Int. Ed.* **2018**, *57*, 14841−14846.

(22) Shimada, S.; Yamazaki, O.; Tanaka, T.; Suzuki, Y.; Tanaka, M. Synthesis and structure of 5,6,7,12-tetrahydrodibenz[c,f][1,5]-azabismocines. *J. Organomet. Chem.* **2004**, *689*, 3012−3023.

(23) Parke, S. M.; Narreto, M. A. B.; Hupf, E.; McDonald, R.; Ferguson, M. J.; Hegmann, F. A.; Rivard, E. Understanding the Origin of Phosphorescence in Bismoles: A Synthetic and Computational Study. *Inorg. Chem.* **2018**, *57*, 7536−7549.

(24) Dognon, J.-P.; Pyykkö, P. Determining nuclear quadrupole moments of Bi and Sb from molecular data. *Phys. Chem. Chem. Phys.* **2023**, *25*, 2758−2761.

(25) Vícha, J.; Novotný, J.; Komorovsky, S.; Straka, M.; Kaupp, M.; Marek, R. Relativistic Heavy-Neighbor-Atom Effects on NMR Shifts: Concepts and Trends Across the Periodic Table. *Chem. Rev.* **2020**, *120*, 7065−7103.

(26) MacMillan, J. W. M.; Marczenko, K. M.; Johnson, E. R.; Chitnis, S. S. Hydrostibination of Alkynes: A Radical Mechanism. *Chem.—Eur. J.* **2020**, *26*, 17134−17142.

(27) Pang, Y.; Leutzsch, M.; Nöthling, N.; Cornella, J. Dihydrogen and Ethylene Activation by a Sterically Distorted Distibene. *Angew. Chem., Int. Ed.* **2023**, *62*, e202302071.

(28) Roy, M.M D.; Omana, A. A.; Wilson, A. S. S.; Hill, M. S.; Aldridge, S.; Rivard, E. Main Group Metal Hydrides. *Chem. Rev.* **2021**, *121*, 12784−12965.

https://doi.org/10.1021/jacs.3c06535
J. Am. Chem. Soc. XXXX, XXX, XXX−XXX